Catalase Deficiency Accelerates Diabetic Renal Injury Through Peroxisomal Dysfunction

Inah Hwang,[1] Jiyoun Lee,[1] Joo Young Huh,[1] Jehyun Park,[1] Hi Bahl Lee,[2] Ye-Shih Ho,[3] and Hunjoo Ha[1]

Mitochondrial reactive oxygen species (ROS) play an important role in diabetes complications, including diabetic nephropathy (DN). Plasma free fatty acids (FFAs) as well as glucose are increased in diabetes, and peroxisomes and mitochondria participate in FFA oxidation in an interconnected fashion. Therefore, we investigated whether deficiency of catalase, a major peroxisomal antioxidant, accelerates DN through peroxisomal dysfunction and abnormal renal FFA metabolism. Diabetes was induced by multiple injections of low-dose streptozotocin into catalase knock-out (CKO) and wild-type (WT) C57BL/6 mice. Murine mesangial cells (MMCs) transfected with catalase small interfering RNA followed by catalase overexpression were used to further elucidate the role of endogenous catalase. Despite equivalent hyperglycemia, parameters of DN, along with markers of oxidative stress, were more accelerated in diabetic CKO mice than in diabetic WT mice up to 10 weeks of diabetes. CKO mice and MMCs showed impaired peroxisomal/mitochondrial biogenesis and FFA oxidation. Catalase deficiency increased mitochondrial ROS and fibronectin expression in response to FFAs, which were effectively restored by catalase overexpression or *N*-acetylcysteine. These data provide unprecedented evidence that FFA-induced peroxisomal dysfunction exacerbates DN and that endogenous catalase plays an important role in protecting the kidney from diabetic stress through maintaining peroxisomal and mitochondrial fitness. ***Diabetes*** **61:728–738, 2012**

Diabetic nephropathy (DN) is the leading cause of end-stage renal disease worldwide and an independent risk factor for cardiovascular morbidity and mortality (1). DN is characterized by albuminuria, decreased glomerular filtration rate, and excessive deposition of extracellular matrix (ECM) leading to glomerular mesangial expansion and tubulointerstitial fibrosis (2–4). Large randomized clinical studies show a causal relationship between hyperglycemia and renal injury in both type 1 (5) and type 2 (6) diabetes. Numerous studies also suggest that hyperglycemia-induced reactive oxygen species (ROS) contribute to the development and progression of DN (7–10).

Plasma free fatty acids (FFAs) are also increased under the diabetic milieu. However, the role of FFA flux in insulin-independent tissues, including the kidney, has been relatively underappreciated compared with the role of glucose flux. In this context, recent studies show that FFAs stimulate ROS through protein kinase C–dependent NADPH oxidase (Nox) in vascular smooth muscle cells and endothelial cells (11) and that FFAs reduce acetylcholine-induced forearm blood flow, which was prevented by vitamin C (12). Oleate has been reported to induce myofibroblast phenotype in mesangial cells through transforming growth factor (TGF)-β1 activation, which suggests that elevated FFAs may induce ECM remodeling and renal fibrosis (13). We have observed previously that oleate-induced ROS upregulate fibronectin (FN) in murine mesangial cells (MMCs) (14).

Peroxisome is an essential organelle for lipid metabolism, as evidenced by increased plasma very long-chain FA in patients with Zellweger syndrome, which is an inherited disease of peroxisomal deficiency (15). During FA β-oxidation, peroxisomes generate H_2O_2, which is mostly decomposed to water and oxygen by catalase (16). Mammalian catalase is a 240-kDa homotetrameric heme-containing protein located exclusively in the peroxisome and abundantly expressed in liver, lungs, and kidneys (17). In a recent study, Elsner et al. (18) reported that overexpression of catalase in the peroxisome, but not in the mitochondria, reduces H_2O_2 production and protects insulin-producing cells from long-chain FA–induced lipotoxicity. These findings indicate that H_2O_2 generated by peroxisomal β-oxidation plays an important role in lipotoxicity under certain conditions. Consistent with this study, when catalase activity in myocardial peroxisomes was inhibited by aminotriazole, a catalase inhibitor, lipids were peroxided and accumulated in the heart (19), leading to a severe cardiac failure (20). Although peroxisomes contain full enzymatic machinery for FA β-oxidation, FA shortened through peroxisomal β-oxidation could be shuttled to mitochondria for complete oxidation. For this reason, peroxisomal metabolism is closely related to mitochondria (21). In this context, absence of catalase could cause impairment of mitochondria as well as peroxisomes (22). Although catalase overexpression attenuated diabetic renal injury (23,24), the role of endogenous catalase in DN and the molecular mechanism linking catalase to lipid flux in renal cells have not been studied.

Therefore, we investigated whether endogenous catalase plays a role in protecting kidney from FFA-induced lipotoxicity under diabetic conditions using catalase null (CKO) mice. We further investigated whether catalase deficiency induces peroxisomal dysfunction leading to mitochondrial dysfunction and lipid accumulation using small interfering (si)RNA-transfected MMCs cultured under phytanic acid (PhA), a branched FA metabolized exclusively in the peroxisome, alone or in combination with high glucose (HG). Transgenic catalase was used to verify the on-target effect of catalase siRNA (siCat).

From the [1]Department of Bioinspired Science, Division of Life and Pharmaceutical Sciences, Center for Cell Signaling and Drug Discovery Research, College of Pharmacy, Ewha Womans University, Seoul, Korea; [2]Kim's Clinic and Dialysis Unit, Myrang, Korea; and the [3]Institute of Environmental Health Sciences, Wayne State University, Detroit, Michigan.
Corresponding author: Hunjoo Ha, hha@ewha.ac.kr.
Received 4 May 2011 and accepted 8 December 2011.
DOI: 10.2337/db11-0584
This article contains Supplementary Data online at http://diabetes.diabetesjournals.org/lookup/suppl/doi:10.2337/db11-0584/-/DC1.

RESEARCH DESIGN AND METHODS

Materials. Reagents for immunohistochemical staining were purchased from DAKO A/S (Glostrup, Denmark), anti–E-cadherin was obtained from BD Biosciences (San Jose, CA), anti-catalase was obtained from Young In Frontier (Seoul, Korea), and other antibodies were obtained from Santa Cruz Biotechnology Inc. (Santa Cruz, CA). FBS was purchased from GIBCO BRL (Gaithersburg, MD), and MitoSOX was obtained from Molecular Probes (Eugene, OR). Other chemicals and tissue culture plates were obtained from Sigma-Aldrich (St. Louis, MO) and Becton Dickinson Labware (Lincoln Park, NJ), respectively, unless otherwise stated.

Animals. Male catalase wild-type (WT) and CKO C57BL/6 J mice (17) were used in this study. All animal experiments were approved by Ewha Womans University Institutional Animal Care and Use Committee. Six-week-old mice were divided into four groups: nondiabetic and diabetic WT mice and nondiabetic and diabetic CKO mice. Diabetes was induced by intraperitoneal injection of streptozotocin (STZ; 50 mg/kg/day) for 5 days and mice were kept up to 10 weeks of diabetes (25). Blood pressure was measured every week by CODA High-Throughout Non-Invasive Tail Blood Pressure system (Kent Scientific Corporation, Torrington, CT).

Cell culture. MMCs were cultured as described previously (26). Subconfluent MMCs were transfected with 20 nmol/L siCat (sense, 5′-CCA GAU ACU CCA AGG CAA ATT-3′; antisense, 5′-UUU GCC UUG GAG UAU CUG GTT-3′) using Lipofectamine RNAiMAX (Invitrogen, Carlsbad, CA) for 24 h. For overexpression experiments, MMCs were transfected with 100 ng p-cytomegalovirus (pCMV)–human catalase (hCat) plasmid (supplied by Professor Sue Goo Rhee, Ewha Womans University) after siRNA transfection for 24 h.

Biochemical data. Blood glucose, urinary creatinine and albumin concentrations, and body weight were measured every 2 weeks. Urine was collected during two consecutive 24-h periods, during which each mouse was individually housed in a metabolic cage with free access to food and water. Blood glucose was measured by the glucose oxidase method, plasma creatinine was measured by Detect X Serum Creatinine Detection Kit (Arbor Assays, Ann Arbor, MI), and plasma FFAs were measured by EnzyChrom Free Fatty Acid Assay Kit (BioAssay Systems, Hayward, CA). Urinary protein was analyzed by Bradford assay and SDS-PAGE (27). The levels of urinary lipid peroxide (LPO) were measured by the thiobarbituric acid method as described previously (28).

Mitochondrial ROS measurement. Mitochondrial ROS were measured using MitoSOX. In brief, after stimulation, the cells were washed and incubated with 2.5 μmol/L MitoSOX for 10 min. The unbound dye was then removed and fluorescence was analyzed using a flow cytometer (BD Biosciences) and visualized by confocal microscopy (Carl Zeiss, Gottingen, Germany).

Morpholometric analysis. In each mouse, quantitative analysis of glomerular volume and fractional mesangial area (FMA) in the glomeruli stained with periodic acid Schiff (PAS) reagent was conducted as described previously (25).

Immunostaining. Immunohistochemistry for nitrotyrosine and FN ED-A was performed as described previously (29) using anti–*N*-nitrotyrosine (1:200) and anti–FN ED-A (1:200). For the detection of peroxin (PEX)5 in MMCs, the cells were fixed with 4% paraformaldehyde for 10 min, incubated with serum-free blocking solution for 15 min, and then reacted with anti-PEX5 (1:200). After washing two times with PBS, the samples were incubated with Alexa Fluor 488–tagged goat anti-mouse IgG (H+L) (1:100) for 1 h. Images were obtained by confocal microscopy (Carl Zeiss).

Real-time PCR. Isolation of total RNA from the whole kidney and MMCs, synthesis of cDNA by reverse transcription, and quantitative real-time PCR were performed as described previously (25). PCR primer sequences are listed in Supplementary Table 1.

Western blot analysis. E-cadherin, α-smooth muscle actin (α-SMA), and FN protein were measured by a standard Western blot analysis as described previously (25), using anti-human E-cadherin (1:5,000), anti-mouse α-SMA (1:10,000), and anti-human FN (1:2,000).

Lipid accumulation. For Oil Red O staining, fixed tissues and cells were washed and incubated with 0.3% Oil Red O for 10 min. After washing with distilled water, images were obtained by microscopy (Carl Zeiss).

Statistical analyses. All results are expressed as mean ± SE. ANOVA was used to assess the differences between multiple groups. If the F statistic was significant, the mean values of each group were compared by Fisher least significant difference method. $P < 0.05$ was considered significant.

RESULTS

Diabetic renal injury was accelerated by catalase deficiency. After multiple injections of low-dose STZ, both diabetic WT and diabetic CKO mice maintained hyperglycemia up to 10 weeks of diabetes, but there was no difference between the two groups (Table 1). The kidney weight (absolute and adjusted) of diabetic CKO mice was significantly increased when compared with diabetic WT mice at both 4 and 10 weeks of diabetes (Table 1). Mean blood pressure (mmHg) was significantly increased from 5 weeks of diabetes, but there was little difference between diabetic WT and diabetic CKO mice (WT: 108 ± 8; diabetic WT: 135 ± 12; diabetic CKO: 140 ± 4 at 10 weeks of diabetes), suggesting that blood pressure did not play a significant role in accelerated renal injury in diabetic CKO mice under our experimental condition.

Urinary protein excretion was gradually increased up to 10 weeks of diabetes and was significantly increased in diabetic CKO compared with diabetic WT mice at both 4 weeks and 10 weeks of diabetes (Fig. 1*A* and *B*). Plasma creatinine levels were also gradually increased in both diabetic groups and were significantly higher in diabetic CKO mice than in diabetic WT mice at 10 weeks of diabetes (Fig. 1*C*). Glomerular volume in both diabetic groups was gradually increased up to 10 weeks of diabetes, and in diabetic CKO mice, glomerular volume and FMA were higher than that of diabetic WT mice at both 4 and 10 weeks of diabetes (Fig. 1*D–F*). It is important to note that glomerular volume and FMA in nondiabetic CKO mice were significantly higher than age-matched nondiabetic WT mice (Supplementary Fig. 1*A* and *B*). These results suggest that catalase deficiency exacerbates renal injury in early diabetes.

Renal fibrosis was accelerated by catalase deficiency. We next measured the pro- and antifibrotic cytokines along with markers of epithelial-to-mesenchymal transition, which is an early event in DN (30). TGF-β1 (Fig. 2*A*), connective tissue growth factor (CTGF) (Fig. 2*B*), α-SMA (Fig. 2*D*) mRNA, and α-SMA protein (Fig. 2*F*) expression levels were significantly increased in diabetic CKO compared with diabetic WT mice at 4 and 10 weeks of diabetes. CTGF and α-SMA expressions in diabetic CKO kidneys were more significantly increased at 10 weeks of diabetes. Conversely, bone morphogenic protein 7 (BMP7)—a renoprotective antifibrotic cytokine—mRNA (Fig. 2*C*), E-cadherin mRNA (Fig. 2*E*), and protein (Fig. 2*G*) expressions in diabetic CKO kidneys were significantly decreased compared with diabetic WT kidneys at both 4 and 10 weeks of diabetes. In nondiabetic CKO kidneys, the expressions of TGF-β1, CTGF, α-SMA, and FN mRNA were significantly

TABLE 1
Characteristics of animals

	4 weeks of diabetes			10 weeks of diabetes		
	WT	WTDM	CKODM	WT	WTDM	CKODM
Body weight (g)	22.8 ± 0.7	19.0 ± 0.9*	23.1 ± 0.9†	28.2 ± 0.5	23.3 ± 0.4*	24.1 ± 0.6*
Kidney weight (g)	0.14 ± 0.01	0.14 ± 0.01	0.17 ± 0.01*†	0.14 ± 0.01	0.18 ± 0.01*	0.23 ± 0.01*†
Kidney-to-body ratio (mg/g)	7.4 ± 0.1	7.6 ± 0.2	7.8 ± 0.1*	5.1 ± 0.2	7.6 ± 0.3*	9.6 ± 0.4*†
Blood glucose (mg/dL)	193 ± 15	362 ± 50*	397 ± 74*	159 ± 7	596 ± 43*	657 ± 27*

Data are mean ± SE of n = 5–7 mice per group. DM, diabetic mice. *$P < 0.05$ vs. WT. †$P < 0.05$ vs. WTDM.

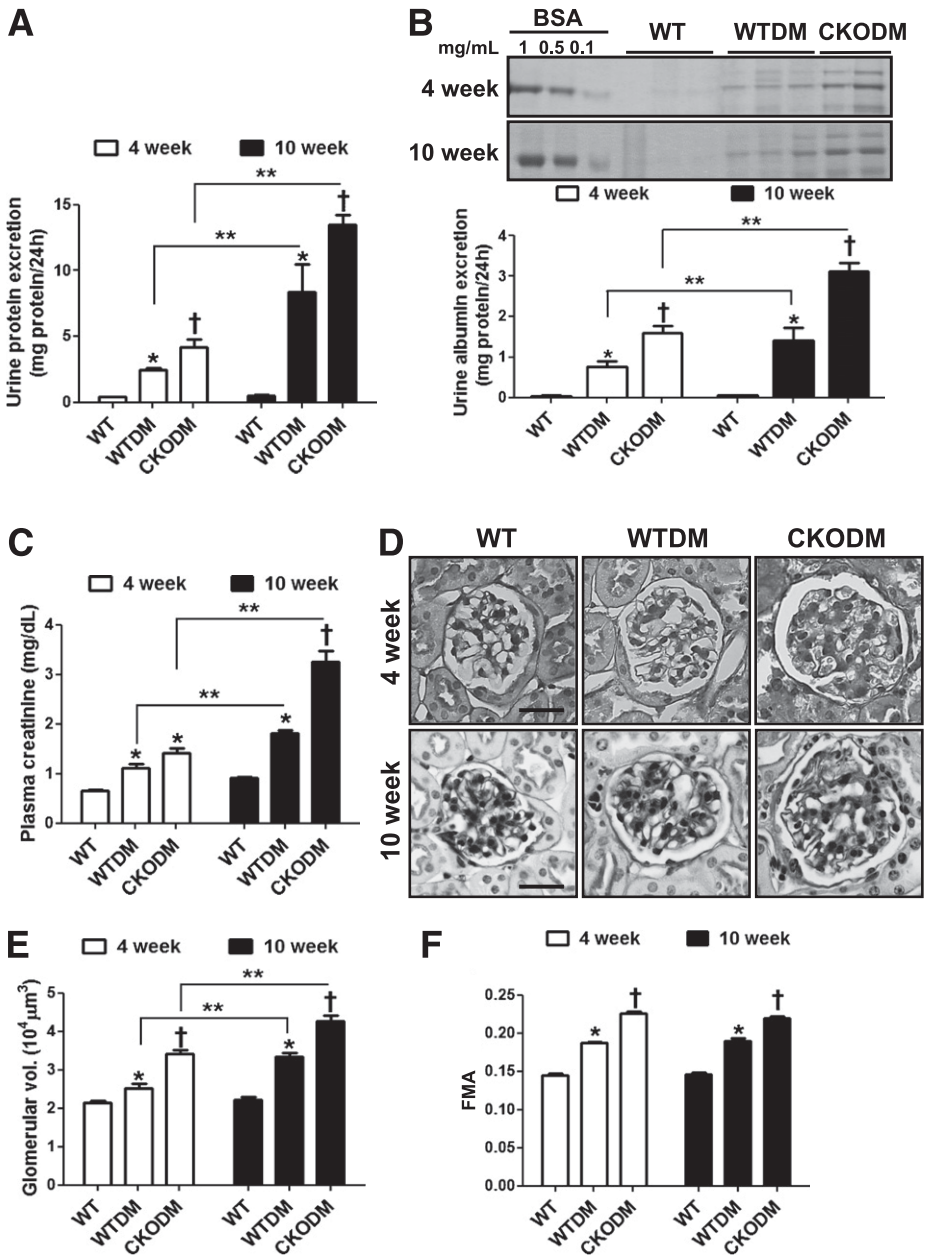

FIG. 1. Diabetic renal injury was accelerated in diabetic CKO mice. At 4 and 10 weeks after the induction of diabetes, parameters of DN were analyzed. *A* and *B*: Urinary protein excretion was measured by Bradford assay (*A*) or SDS-PAGE (*B*). *C*: Plasma creatinine was measured by Detect X Serum Creatinine Detection Kit. *D–F*: The kidneys were fixed, cut into 4-μm sections, and stained with PAS reagent (*D*). Scale bar, 20 μm; magnification ×630. After PAS staining, the glomerular volume (*E*) and FMA (*F*) were analyzed using Image Pro Plus (50 glomeruli per animal). WT, nondiabetic control mice; WTDM, STZ-induced diabetic WT mice; CKODM, STZ-induced diabetic CKO mice. Data are mean ± SE of n = 7–8 mice per group. *P < 0.05 vs. WT; †P < 0.05 vs. WTDM at the same duration of diabetes; **P < 0.05 between two groups.

upregulated, while BMP7 and E-cadherin mRNA were significantly downregulated compared with nondiabetic WT kidneys (Supplementary Fig. 1*G*).

Consistently, FN mRNA and protein expressions in diabetic CKO kidneys were significantly higher than in diabetic WT kidneys. The increase in FN protein levels in both diabetic WT and CKO kidneys were more evident at 10 weeks of diabetes than at 4 weeks (Fig. 3*A* and *B*). Immunohistochemical analysis at 4 weeks of diabetes confirmed that FN ED-A was strongly expressed in the glomeruli of diabetic WT mice and in the tubules and glomeruli of diabetic CKO mice (Fig. 3*C*). Masson trichrome staining showed significantly increased collagen accumulation in diabetic WT kidneys, which was further increased in diabetic CKO kidneys at 10 weeks of diabetes (Fig. 3*D*). These results show that catalase deficiency accelerates renal fibrosis in early diabetes.

Upregulated antioxidative defense mechanisms in diabetic kidneys were blunted by catalase deficiency. Catalase null state was confirmed by real-time PCR in the CKO kidneys (Supplementary Fig. 2*A*). In diabetic WT kidneys, the mRNA levels of antioxidant enzymes, including catalase, glutathione peroxidase-1 (GPx1), peroxiredoxin (Prx)1, Prx5, superoxide dismutase (SOD)1, SOD2, and sulfiredoxin-1, were significantly upregulated compared with nondiabetic WT kidneys (Supplementary Fig. 2*A–G*).

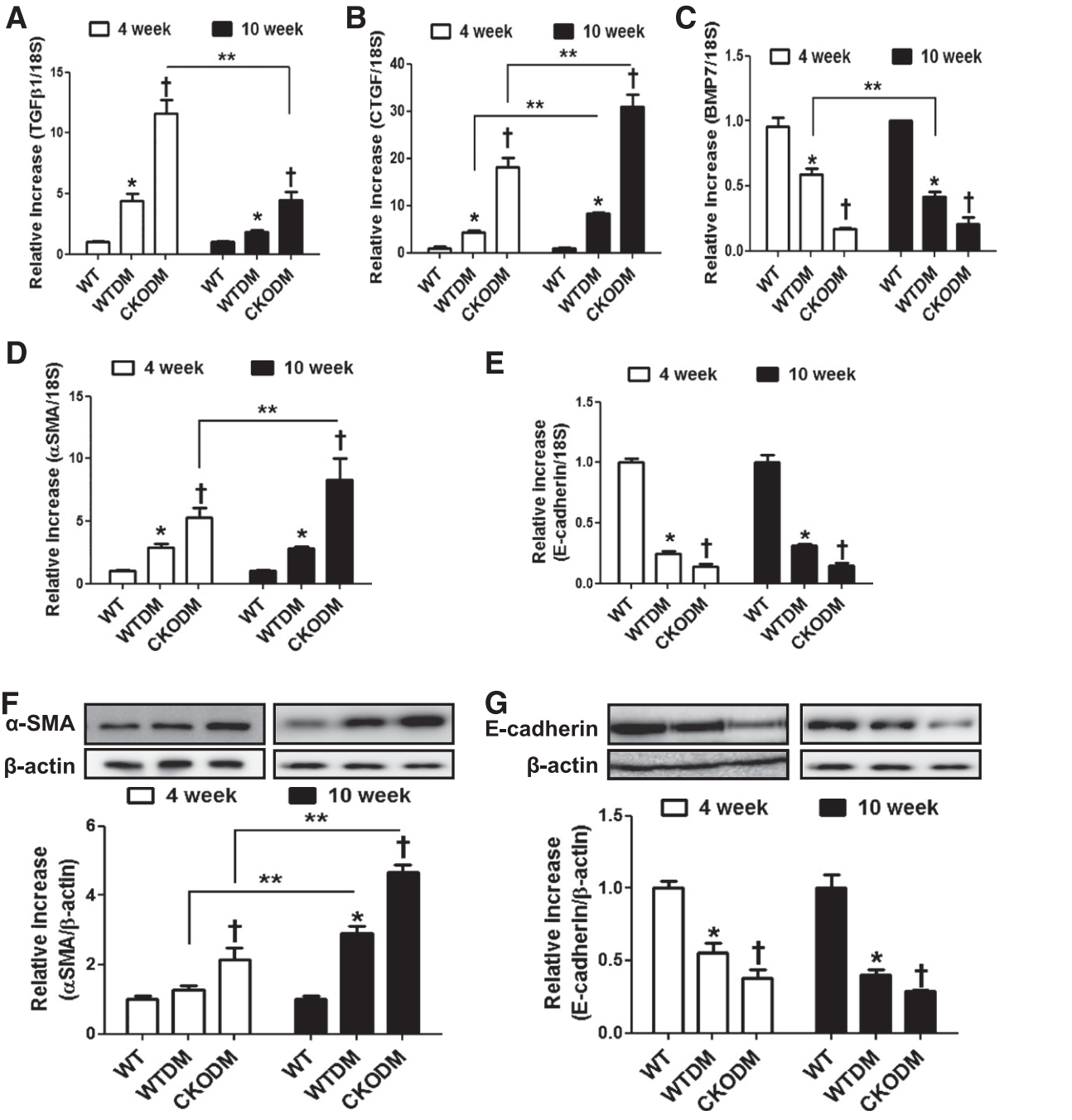

FIG. 2. The profibrotic pathway was accelerated in diabetic CKO mice. At 4 and 10 weeks after the induction of diabetes, mRNA and protein samples were taken from whole kidney. *A–E*: Renal TGF-β1 (*A*), CTGF (*B*), BMP7 (*C*), α-SMA (*D*), and E-cadherin (*E*) mRNA expressions were analyzed by real-time PCR. *F* and *G*: α-SMA (*F*) and E-cadherin (*G*) protein expressions were analyzed by Western blot. WT, nondiabetic control mice; WTDM, STZ-induced diabetic WT mice; CKODM, STZ-induced diabetic CKO mice. Data are mean ± SE of n = 7–8 mice per group. *$P < 0.05$ vs. WT; †$P < 0.05$ vs. WTDM at the same duration of diabetes; **$P < 0.05$ between two groups.

Moreover, Prx1 and Prx5 mRNA expressions in nondiabetic CKO kidneys were significantly higher than in nondiabetic WT kidneys. Unexpectedly, upregulated expressions of antioxidant enzymes were blunted in diabetic CKO kidneys. In fact, renal expressions of GPx1, Prx5, SOD1, SOD2, and sulfiredoxin-1 mRNA in diabetic CKO mice were significantly lower than in diabetic WT mice.

Oxidative stress was higher in diabetic CKO kidneys than in diabetic WT kidneys. Renal Nox4 plays an important role in increased oxidative stress leading to DN (31), and H_2O_2 upregulates Nox4 mRNA expression in MMCs (32). We, therefore, measured Nox4 mRNA expression in addition to urinary LPO and nitrotyrosine accumulation as markers of renal oxidative stress. Renal Nox4 mRNA (Fig. 4*A*) expression, urinary LPO (Fig. 4*B*), and renal nitrotyrosine accumulation (Fig. 4*C* and *D*) were higher in diabetic CKO mice than in diabetic WT mice at 4 weeks of diabetes and were continuously increased in diabetic CKO mice up to 10 weeks. These results, together with the mRNA expression profile of antioxidant enzymes

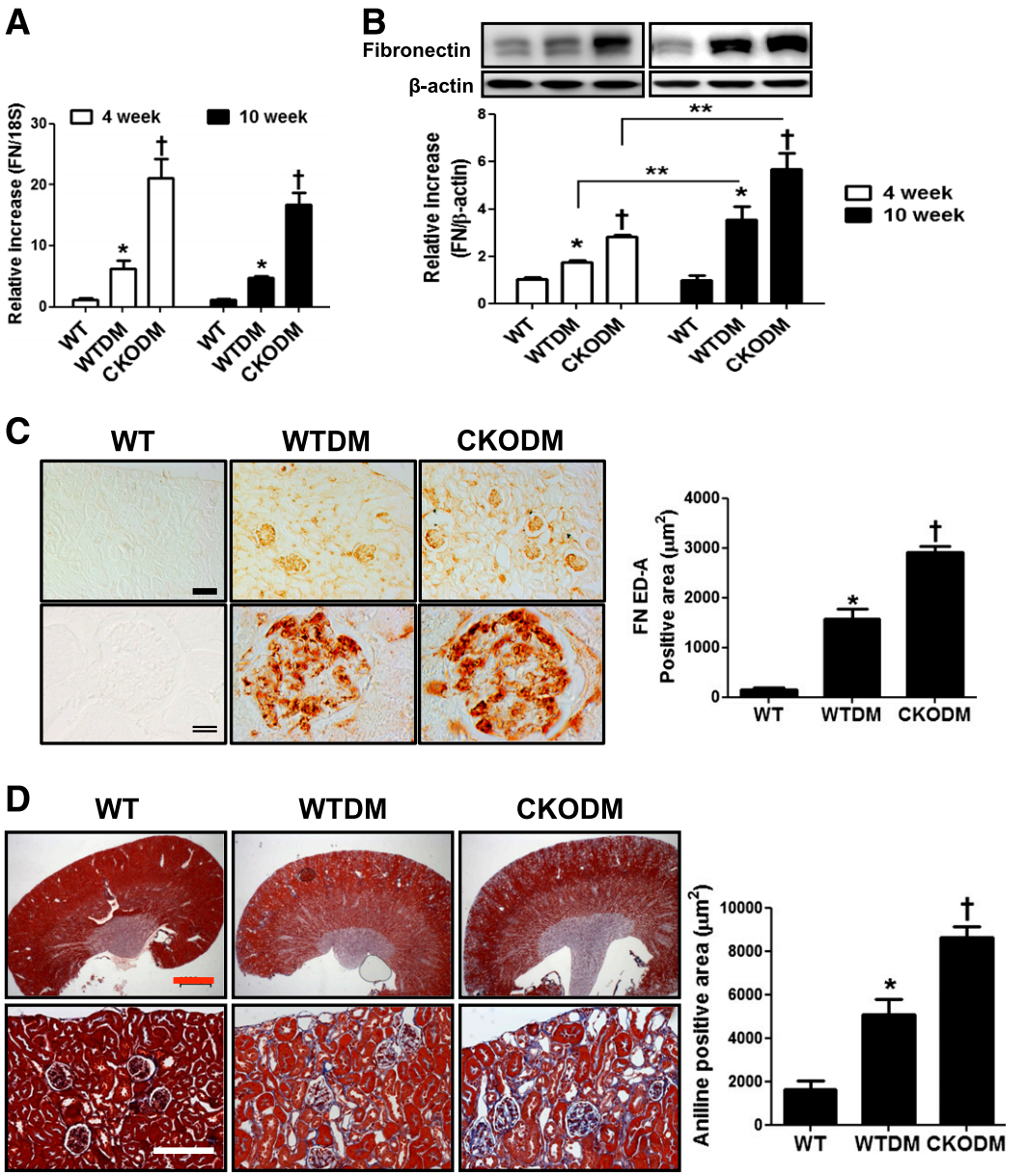

FIG. 3. ECM expression was further increased in diabetic CKO kidneys. *A* and *B*: Renal FN mRNA (*A*) and protein (*B*) expressions at 4 and 10 weeks after the induction of diabetes. *C*: The renal tissues of 4 weeks of diabetes were immunostained with anti–FN ED-A (1:200; *left*), and FN ED-A positive area was quantified by using ImageJ software (*right*; 15 pictures per animal). Single scale bar, 100 μm; magnification ×200. Double scale bar, 20 μm; magnification ×630. *D*: Renal collagen was measured by Masson trichrome staining at 10 weeks after the induction of diabetes (*left*) and quantified (*right*; 15 pictures per animal). The upper and lower pictures are magnification ×12.5 (scale bar, 1 mm) and ×630 (scale bar, 20 μm), respectively. WT, nondiabetic control mice; WTDM, STZ-induced diabetic WT mice; CKODM, STZ-induced diabetic CKO mice. Data are mean ± SE of n = 7–8 mice per group. *$P < 0.05$ vs. WT; †$P < 0.05$ vs. WTDM at the same duration of diabetes; **$P < 0.05$ between two groups. (A high-quality digital representation of this figure is available in the online issue.)

in diabetic CKO kidneys, demonstrate that renal oxidative stress is greatly increased in diabetes by catalase deficiency.

Catalase deficiency disrupted renal peroxisomal biogenesis. We investigated peroxisomal biogenesis as the first step in a mechanistic study of the relationships among catalase, peroxisome, oxidative stress, and DN. Plasma FFAs were significantly upregulated in both diabetic WT and diabetic CKO mice compared with control WT at 4 weeks and further increased in diabetic CKO at 10 weeks of diabetes (Fig. 5*A*). Renal expressions of peroxisomal biogenesis markers including, PEX5, PEX11-α, and ATP-binding cassette member 3 (Abcd3), were significantly higher in diabetic WT mice at 4 weeks but lower at 10 weeks compared with nondiabetic WT mice (Fig. 5*B–E*). In diabetic CKO kidneys, these peroxisomal biogenesis markers were significantly decreased compared with diabetic WT kidneys at both 4 and 10 weeks (Fig. 5*B–E*).

To investigate a direct role of endogenous catalase in the progression of DN, we used MMCs transfected with siCat. siCat decreased the endogenous catalase level down to 40% of basal in MMCs and was restored by additional catalase expression using pCMV-hCAT (Fig. 5*F*). PEX5, PEX11-α, and Abcd3 mRNA expressions were significantly upregulated by 100 μmol/L PhA with or without 30 mmol/L D-glucose (HG) for 4 h in MMCs, but these increases were inhibited by catalase knock-down (Fig. 5*G* and *H* and

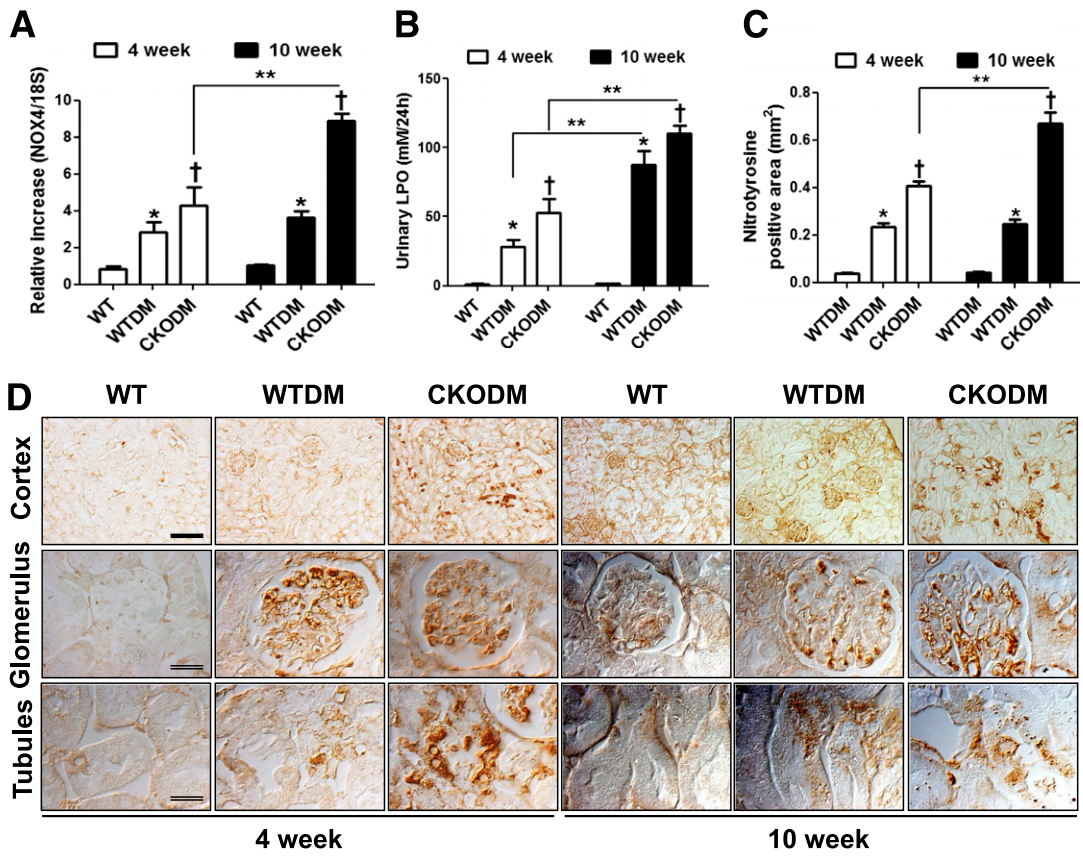

FIG. 4. Oxidative stress was exacerbated in diabetic CKO kidneys. *A*: At 4 and 10 weeks after the induction of diabetes, renal Nox4 mRNA expression was measured by real-time PCR. *B*: Urinary LPO was assessed by thiobarbituric acid assay. *C* and *D*: Renal nitrotyrosine accumulation was measured by immunohistochemistry using anti-nitrotyrosine (1:200) (*C*) and quantified by using ImageJ (15 pictures per animal) (*D*). Single scale bar, 100 μm; magnification ×200. Double scale bar, 20 μm; magnification ×630. WT, nondiabetic control mice; WTDM, STZ-induced diabetic WT mice; CKODM, STZ-induced diabetic CKO mice. Data are mean ± SE of n = 7–8 mice per group. *P < 0.05 vs. WT; †P < 0.05 vs. WTDM at the same duration of diabetes; **P < 0.05 between two groups. (A high-quality digital representation of this figure is available in the online issue.)

Supplementary Fig. 3*B*–*E*). Peroxisomal biogenesis markers inhibited by catalase deficiency were restored by hCAT transfection, confirming the on-target effect of siCat. *N*-acetylcysteine (NAC) also effectively restored the inhibition of peroxisomal biogenesis induced by catalase deficiency. Decreased PEX5 expression was further confirmed by Western blot and immunocytochemistry (Fig. 5*J* and *I*). It is interesting that 100 μmol/L H_2O_2 treatment significantly increased peroxisomal biogenesis, but not at >250 μmol/L (Supplementary Fig. 3*A*). These results suggest that FFA-induced oxidative stress requires catalase for peroxisomal fitness, but severe oxidative stress, such as H_2O_2 at levels >250 μmol/L or catalase deficiency under diabetic conditions, disrupts adaptive peroxisomal biogenesis.

Catalase deficiency disrupted renal mitochondrial biogenesis. To investigate whether catalase deficiency induces the accumulation of mitochondrial ROS, we measured mitochondrial superoxide anion levels using MitoSOX. MitoSOX-sensitive ROS were significantly increased by PhA with or without HG treatment and further increased by catalase knock-down (Fig. 6*A* and *B*). Accelerated mitochondrial ROS in catalase knock-down cells were effectively prevented by hCAT transfection or by NAC treatment. MitoSOX levels were not significantly different between PhA alone and PhA plus HG treatment.

To determine if catalase deficiency induced impaired mitochondrial fitness, we measured cytochrome b mRNA level, a marker of mitochondrial biogenesis, in MMCs and diabetic animals. As a result of increased mitochondrial ROS, catalase deficiency inhibited PhA with or without HG–induced cytochrome b mRNA expression, which was restored by hCAT transfection or NAC treatment (Fig. 6*C*). The PhA plus HG–induced cytochrome b mRNA level was higher than PhA treatment alone (Fig. 6*D*). Similar to peroxisomal biogenesis markers, cytochrome b mRNA level was higher in diabetic WT kidneys at 4 weeks but lower at 10 weeks of diabetes compared with nondiabetic WT kidneys (Fig. 6*E*). In diabetic CKO kidneys, cytochrome b mRNA level was significantly decreased at both 4 and 10 weeks compared with diabetic WT kidneys (Fig. 6*E*). These results suggest that catalase deficiency increases mitochondrial ROS, which might play a role in dysregulation of mitochondrial biogenesis.

Catalase deficiency induced renal lipid accumulation. To determine if the impaired peroxisomal and mitochondrial biogenesis induced by catalase deficiency under the diabetic milieu affected renal lipid metabolism, we measured the peroxisomal and mitochondrial β-oxidation and lipid accumulation. mRNA expressions of acyl-CoA oxidase (ACO), a key enzyme of peroxisomal β-oxidation, and carnitine palmitoyltransferase (CPT)1-α, a regulator of long-chain FA entry to mitochondria, were significantly decreased in diabetic WT compared with control WT kidneys and were further decreased in diabetic CKO kidneys at both 4 and 10 weeks of diabetes (Fig. 7*A*). Oil Red O staining

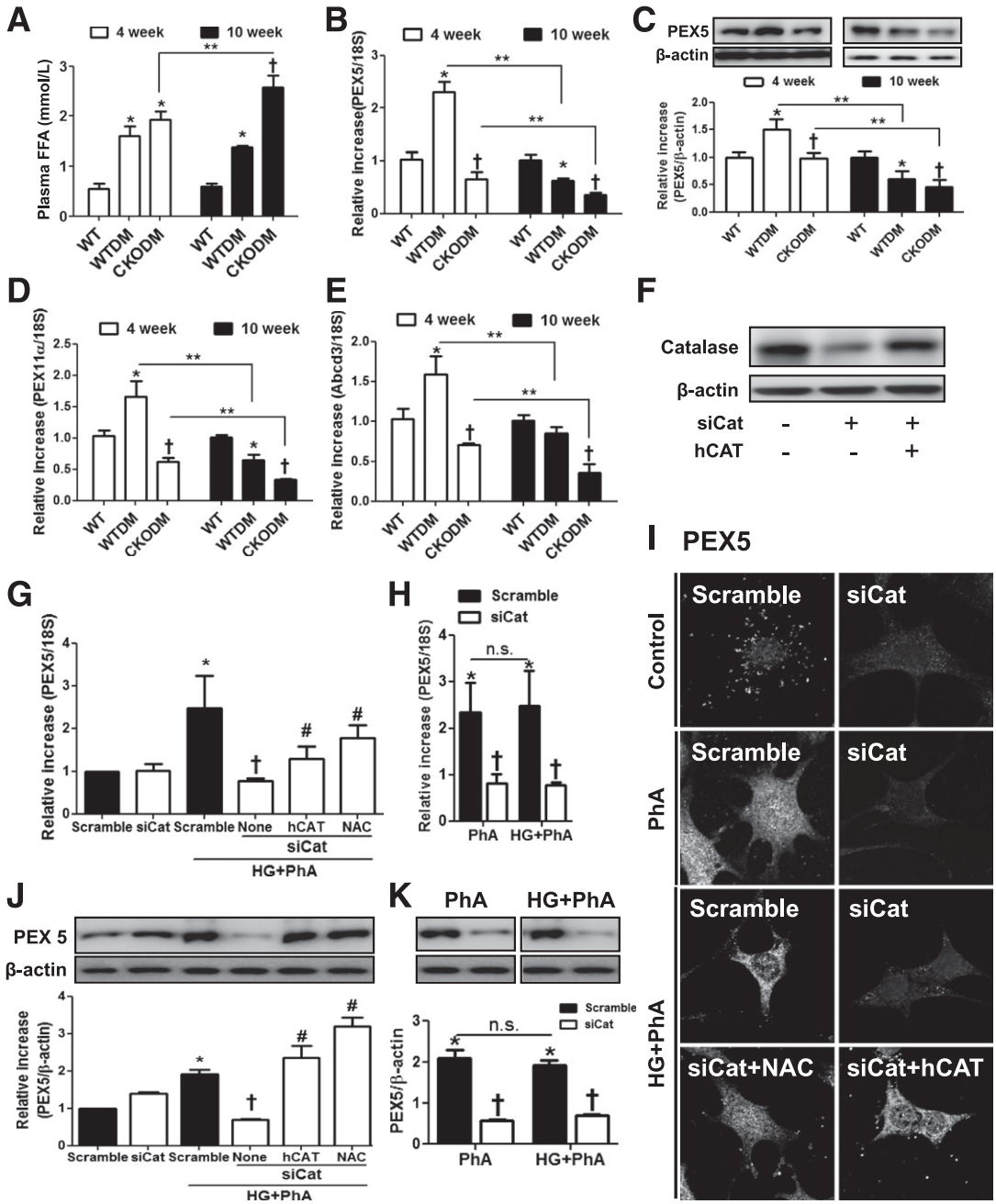

FIG. 5. Catalase deficiency impaired peroxisomal biogenesis. *A*: At 4 and 10 weeks after the induction of diabetes, plasma FFAs (*A*) were measured as described in RESEARCH DESIGN AND METHODS. B–E: Renal PEX5 (*B*), PEX11-α (*D*), and Abcd3 (*E*) mRNA expressions were analyzed by real-time PCR. PEX5 protein (*C*) was measured by Western blot analysis. WT, nondiabetic control mice; WTDM, STZ-induced diabetic WT mice; CKODM, STZ-induced diabetic CKO mice. Data are mean ± SE of n = 7–8 mice per group. *$P < 0.05$ vs. WT; †$P < 0.05$ vs. WTDM at the same duration of diabetes; **$P < 0.05$ between two groups. *F*: The efficacy of siCat or hCAT in MMCs was analyzed by Western blot. MMCs were transfected with 20 nmol/L siCat or scramble siRNA for 24 h. Remaining siRNA were washed and then transfected with 100 ng hCAT. *G–K*: MMCs were then cultured under PhA±HG for 4 h (RNA) or 24 h (protein). NAC (5 mmol/L) was pretreated for 24 h where indicated. PEX5 mRNA (*G* and *H*) was measured by real-time PCR, and protein (*J* and *K*) was measured by Western blot. After 24 h, MMCs were fixed and then immunostained with anti-PEX5 (1:300) (*I*). Magnification ×630. siCat, MMCs transfected with 20 nmol/L siCat; hCAT, MMCs transfected with 100 ng pCMV-hCat; NAC (5 mmol/L); HG (30 mmol/L D-glucose); PhA (100 μmol/L). Data are mean ± SE of n = 4 experiments in the cell culture study. *$P < 0.05$ vs. scramble siRNA-transfected cells; †$P < 0.05$ vs. scramble siRNA-transfected cells cultured under PhA±HG; #$P < 0.05$ vs. siCat-transfected cells cultured under PhA+HG; n.s. not significant between two groups.

revealed more lipid droplets in the glomeruli and tubules of diabetic WT mice than in nondiabetic WT mice at 10 weeks of diabetes (Fig. 7*B*). In diabetic CKO mice, lipid droplets in the glomeruli were significantly higher than in diabetic WT mice (Fig. 7*B*).

In MMCs, ACO, and CPT1-α, mRNA expressions were significantly upregulated by PhA with or without HG, and these were inhibited by catalase knock-down (Fig. 7*C*). Again, hCAT transfection or NAC treatment restored the decreased ACO and CPT1-α mRNA expressions in catalase knock-down cells (Fig. 7*C*). ACO mRNA levels were not different between MMCs treated with PhA alone versus PhA plus HG, but CPT1-α mRNA levels were higher in MMCs treated with PhA alone compared with PhA plus HG

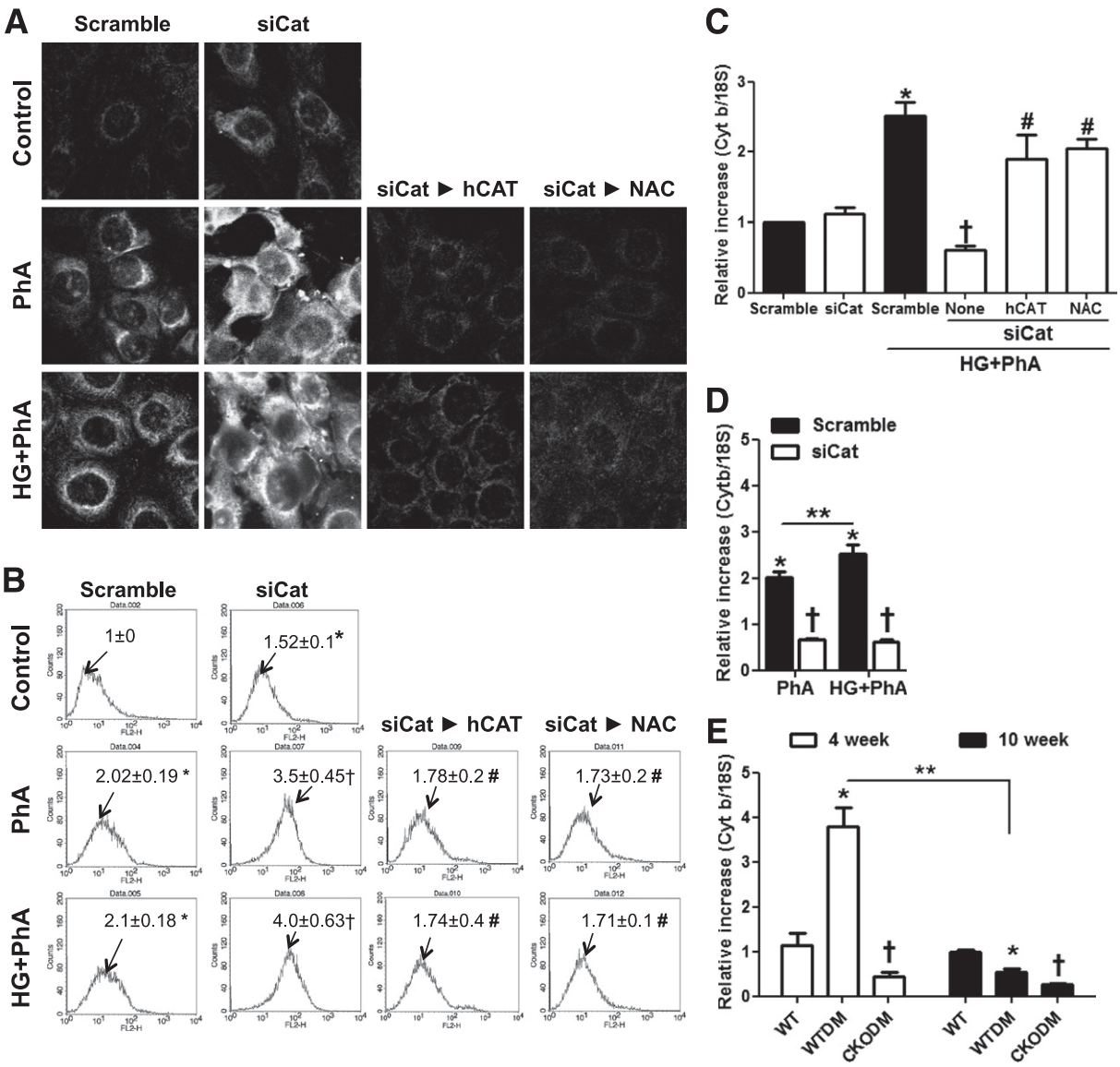

FIG. 6. Catalase deficiency induced accumulation of mitochondrial ROS and impairment of mitochondrial biogenesis. *A* and *B*: Mitochondrial ROS were measured by MitoSOX. After transfection with siCat or scramble siRNA, cells were cultured under PhA±HG for 1 h and then loaded with 2.5 μmol/L MitoSOX for 10 min. The intensity of MitoSOX was assessed by confocal microscope (*A*) and flow cytometry (*B*). Magnification of confocal image is ×630; numbers on histogram plot are means as ratio to control. *C* and *D*: Cytochrome b (Cyt b) mRNA expression was measured in MMCs cultured under PhA±HG for 4 h. siCat, MMCs transfected with 20 nmol/L siCat; hCAT, MMCs transfected with 100 ng pCMV-hCat; NAC (5 mmol/L); HG (30 mmol/L D-glucose); PhA (100 μmol/L). Data are mean ± SE of n = 4 experiments in the cell culture study. *P < 0.05 vs. scramble siRNA-transfected cells; †P < 0.05 vs. scramble siRNA-transfected cells cultured under PhA+HG; #P < 0.05 vs. siCat-transfected cells cultured under PhA+HG; **P < 0.05 between two groups. *E*: Cyt b mRNA expression was measured in animals at 4 and 10 weeks after the induction of diabetes. WT, nondiabetic control mice; WTDM, STZ-induced diabetic WT mice; CKODM, STZ-induced diabetic CKO mice. Data are mean ± SE of n = 7–8 mice per group. *P < 0.05 vs. WT; †P < 0.05 vs. WTDM at the same duration of diabetes; **P < 0.05 between two groups.

(Fig. 7*C*). Oil Red O staining showed significantly increased lipid droplets in catalase knock-down cells in response to PhA plus HG, and these were effectively inhibited by NAC treatment (Fig. 7*D*).

FN mRNA and protein expressions were significantly increased in MMCs cultured under PhA plus HG, which was more evident than PhA treatment alone, and were further increased in catalase knock-down cells (Fig. 7*E* and *F*). Induction of FN in catalase deficiency was significantly inhibited by hCAT transfection or NAC treatment (Fig. 7*E* and *F*). These results suggest that catalase deficiency impairs peroxisomal and mitochondrial β-oxidation, leading to lipid and ECM accumulations.

DISCUSSION

This study provides experimental evidence that endogenous catalase plays an important role in renal redox regulation and function under diabetic conditions. Despite equivalent hyperglycemia between diabetic WT and diabetic CKO mice, parameters of DN together with plasma FFAs were significantly upregulated in diabetic CKO mice. These accelerations were accompanied by increased urinary LPO and renal nitrotyrosine accumulation in diabetic CKO mice, confirming that increased ROS in diabetic CKO mice are associated with accelerated diabetic renal injury.

It should be noted that the compensatory increase of antioxidant enzymes observed in diabetic WT kidneys was

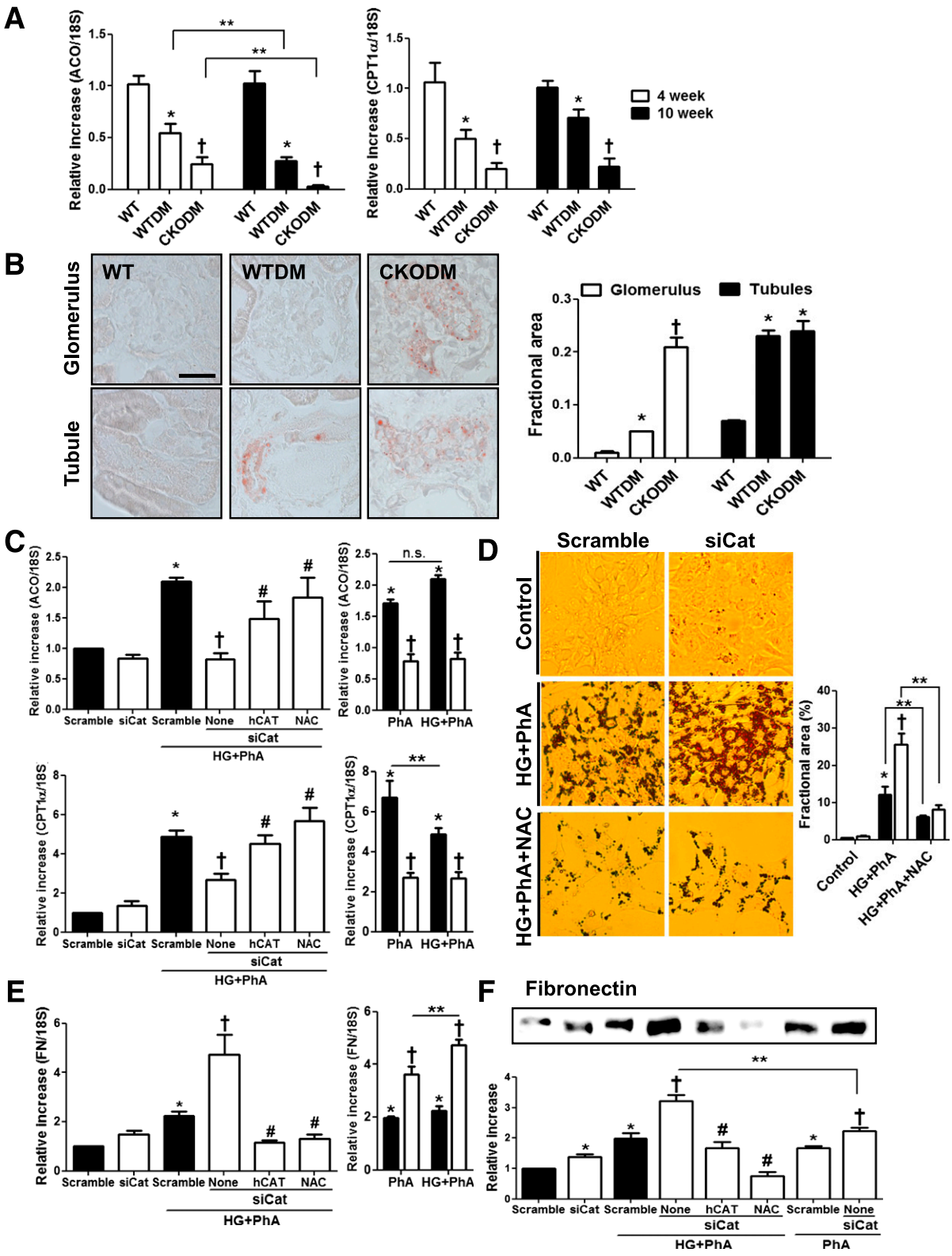

FIG. 7. Catalase deficiency induced renal lipid accumulation. *A*: Renal ACO and CPT1-α mRNA expression were analyzed by real-time PCR. *B*: The renal lipids were detected by Oil Red O staining and quantified using ImageJ software (15 pictures per animal). Scale bar, 20 μm; magnification ×630. WT, nondiabetic control mice; WTDM, STZ-induced diabetic WT mice; CKODM, STZ-induced diabetic CKO mice. Data are mean ± SE of n = 7–8 mice per group. *$P < 0.05$ vs. WT; †$P < 0.05$ vs. WTDM at the same duration of diabetes; **$P < 0.05$ between two groups. *C*: ACO and CPT1-α mRNA expressions were measured in MMCs cultured under PhA±HG for 4 h. *D*: Scramble- or siCat-transfected MMCs were cultured under PhA+HG at presence or absence of NAC for 24 h. Lipid droplets in MMCs were detected by Oil Red O staining and quantified using ImageJ (mean of 10 cells per picture, 5 pictures per group). Magnification ×400. *E*: FN mRNA was measured in MMCs cultured under PhA±HG for 4 h. *F*: Secreted FN in the media of MMCs cultured under PhA±HG for 24 h was measured by Western blot. siCat, MMCs transfected with 20 nmol/L siCat; hCAT, MMCs transfected with 100 ng pCMV-hCat; NAC (5 mmol/L); HG (30 mmol/L D-glucose); PhA (100 μmol/L). Data are mean ± SE of n = 4 experiments in the cell culture study. *$P < 0.05$ vs. scramble siRNA-transfected cells; †$P < 0.05$ vs. scramble siRNA-transfected cells cultured under PhA±HG; #$P < 0.05$ vs. siCat-transfected cells cultured under PhA+HG; **$P < 0.05$ between two groups; n.s. not significant between two groups. (A high-quality digital representation of this figure is available in the online issue.)

attenuated in diabetic CKO kidneys. Although the underlying mechanism is unclear, catalase deficiency might have inhibited Nrf2 expression in diabetic kidneys, for in chronic obstructive pulmonary disease (33), severe oxidative stress inhibits Nrf2, which is the primary transcription factor responsible for upregulation of oxidative responses. In this connection, diabetic renal injury was enhanced in Nrf2 null mice (34); however, not all endogenous antioxidant enzymes play equal roles in diabetic kidneys. For example, GPx1 deficiency rendered similar diabetic renal injury in WT mice (35).

Therefore, it is important to delineate the pathogenic mechanism involved in accelerated diabetic renal injury by catalase deficiency. Accordingly, we attempted to determine whether catalase deficiency disturbs peroxisomal biogenesis, leading to increased mitochondrial ROS and lipid accumulation observed in DN. Peroxisomes undergo reorganization in response to metabolic demands for FA β-oxidation under increased FFAs (21,36). In our in vivo and in vitro study, PEX5, PEX11-α, and Abcd3 mRNA expressions were upregulated in 4 weeks of diabetic WT kidneys and MMCs cultured under PhA with or without HG but not in diabetic CKO kidneys and catalase knock-down MMCs. We also observed increased peroxisomal biogenesis markers in response to 100 μmol/L H_2O_2, but not >250 μmol/L, suggesting context-dependent ROS effects (37). In the case of mitochondria, under oxidative/metabolic stress, initial adaptive increase in mitochondrial biogenesis takes place, while excessive ROS can result in mitochondrial damage (38). Likewise, H_2O_2 produced during FA β-oxidation may increase peroxisomal biogenesis–related genes to meet its metabolic demand, but H_2O_2 above a threshold by catalase deficiency may result in peroxisomal damage. NAC and additional catalase using hCAT transfection confirmed that ROS inhibition results in restoration of peroxisomal biogenesis in catalase knock-down cells. Measurement of in situ H_2O_2 in kidneys by using recently developed methods (39) would be needed to assess the effects in vivo. In addition, although the selectivity of siCat was confirmed partly by hCAT transfection, use of primary MMCs from CKO mice is needed.

Short- and medium-chain FA derived from the diet are exclusively degraded in the mitochondria, whereas peroxisomes catalyze very long-chain FA or branched-chain FA (40). This specifically implies that there would be a metabolic interconnection between the two organelles. Indeed, mitochondrial abnormalities were described in PEX5-deficient mice (41) and patients with Zellweger syndrome (42). In addition, Elsner et al. (18) showed that accumulated H_2O_2 in the mitochondria was reduced by overexpression of peroxisomal catalase in insulin-producing cells. Consistently, the MitoSOX experiment clearly showed that basal as well as PhA-induced mitochondrial ROS were significantly upregulated in catalase knock-down cells. It is notable that mitochondrial ROS, as well as markers of peroxisomal biogenesis (PEX5, PEX11-α, and Abcd3) and peroxisomal β-oxidation (ACO), were significantly increased by PhA treatment alone, which were not significantly different from PhA plus HG treatment, suggesting that PhA plays an important role in the regulation of mitochondrial ROS, peroxisomal biogenesis, and β-oxidation. We next evaluated whether ROS-induced mitochondrial biogenesis was also impaired by catalase deficiency. As expected, mitochondrial biogenesis estimated by cytochrome b expression (Fig. 6*C* and *D*) and mitochondrial DNA and PGC1-α expression (data not shown) were upregulated in MMCs cultured under PhA with or without HG, which were inhibited in catalase knock-down cells. Again, NAC and hCAT transfection restored inhibitory effects of catalase deficiency, suggesting that mitochondria also are damaged at higher levels of ROS. These observations suggest that peroxisomal impairment under catalase deficiency may result in overexpression of mitochondrial ROS and mitochondrial impairment.

Finally, we determined whether peroxisomal and mitochondrial disruption of catalase deficiency influenced lipid metabolism in diabetic kidneys. In contrast to increased peroxisomal/mitochondrial biogenesis at 4 weeks of diabetes, ACO and CPT1-α mRNA expressions were significantly decreased in both diabetic groups, and a greater decrease was observed in diabetic CKO kidneys than in diabetic WT kidneys. Although discrepancies between peroxisomal/mitochondrial biogenesis and β-oxidation at 4 weeks of diabetes are not clear, decreased ACO mRNA in diabetic kidneys has been previously observed (43). It is conceptually supposed that in early diabetes, increased FFAs induce both peroxisomal/mitochondrial biogenesis and β-oxidation. However, when ROS are increased with development of diabetes, β-oxidation is downregulated. We observed that ACO and CPT1-α mRNA expressions were increased in response to PhA with or without HG in control MMCs, but these were inhibited in catalase knock-down cells. We also observed that 100 μmol/L H_2O_2 decreased ACO mRNA expressions but increased peroxisomal biogenesis markers (Supplementary Fig. 3*A* and *F*), suggesting that there might be different thresholds for H_2O_2 concentration between biogenesis and β-oxidation. However, further increased ROS in 10 weeks of diabetes inhibited both biogenesis and β-oxidation. Consistent with decreased β-oxidation, lipid droplets were increased in diabetic CKO kidneys and in catalase knock-down cells cultured under PhA plus HG, which were effectively inhibited by NAC. Therefore, increased ROS in catalase deficiency impair peroxisomal/mitochondrial FA oxidation and subsequently increase lipid accumulation, which might induce renal injury, represented by FN expression in MMCs and diabetic kidney. To the best of our knowledge, this is the first study to focus on peroxisomal dysfunction as a cause of redox dysregulation leading to diabetes complications under catalase deficiency. In summary, the present data provide evidence that FFA-induced peroxisomal dysfunction exacerbates diabetic renal injury and that endogenous catalase is an important antioxidant protecting the kidney through maintaining peroxisomal and mitochondrial fitness under diabetic stress. Further studies elucidating the renoprotective pharmacological and molecular methods to restore peroxisomal biogenesis will provide new insight into the therapeutic strategy against diabetic renal injury.

ACKNOWLEDGMENTS

This work was supported by National Research Foundation grants 2011-0006244 and R31-2008-000-10010-0 funded by the Korean Ministry of Education, Science, and Technology; the second stage of the Brain Korea 21 Project; and RP-Grant 2009 (2009-1949-1-1) from Ewha Womans University to J.P.

No potential conflicts of interest relevant to this article were reported.

I.H. researched data and wrote the manuscript. J.L. and J.P. researched data. J.Y.H. and H.B.L. contributed to

discussion. Y.-S.H. created the CKO mice. H.H. contributed to discussion and reviewed and edited the manuscript. H.H. is the guarantor of this work and, as such, had full access to all the data in the study and takes responsibility for the integrity of the data and the accuracy of the data analysis.

Parts of this study were presented in abstract form at the 44th Annual Meeting of the American Society of Nephrology (abstract TH-PO541), Philadelphia, Pennsylvania, 8–13 November 2011, and at the XLVII ERA-EDTA Congress (abstract 451358), Munich, Germany, 25–28 June 2010.

The authors thank Professors Sue Goo Rhee and Hyun-Ae Woo at Ewha Womans University for supplying CKO mice and pCMV-hCat.

REFERENCES

1. Sarnak MJ, Levey AS, Schoolwerth AC, et al.; American Heart Association Councils on Kidney in Cardiovascular Disease, High Blood Pressure Research, Clinical Cardiology, and Epidemiology and Prevention. Kidney disease as a risk factor for development of cardiovascular disease: a statement from the American Heart Association Councils on Kidney in Cardiovascular Disease, High Blood Pressure Research, Clinical Cardiology, and Epidemiology and Prevention. Circulation 2003;108:2154–2169
2. Mauer SM, Steffes MW, Ellis EN, Sutherland DE, Brown DM, Goetz FC. Structural-functional relationships in diabetic nephropathy. J Clin Invest 1984;74:1143–1155
3. Lane PH, Steffes MW, Fioretto P, Mauer SM. Renal interstitial expansion in insulin-dependent diabetes mellitus. Kidney Int 1993;43:661–667
4. Gilbert RE, Cooper ME. The tubulointerstitium in progressive diabetic kidney disease: more than an aftermath of glomerular injury? Kidney Int 1999;56:1627–1637
5. The Diabetes Control and Complications Trial Research Group. The effect of intensive treatment of diabetes on the development and progression of long-term complications in insulin-dependent diabetes mellitus. N Engl J Med 1993;329:977–986
6. UK Prospective Diabetes Study (UKPDS) Group. Intensive blood-glucose control with sulphonylureas or insulin compared with conventional treatment and risk of complications in patients with type 2 diabetes (UKPDS 33). Lancet 1998;352:837–853
7. Lee HB, Yu MR, Yang Y, Jiang Z, Ha H. Reactive oxygen species-regulated signaling pathways in diabetic nephropathy. J Am Soc Nephrol 2003;14 (Suppl. 3):S241–S245
8. Nishikawa T, Araki E. Impact of mitochondrial ROS production in the pathogenesis of diabetes mellitus and its complications. Antioxid Redox Signal 2007;9:343–353
9. Forbes JM, Coughlan MT, Cooper ME. Oxidative stress as a major culprit in kidney disease in diabetes. Diabetes 2008;57:1446–1454
10. Giacco F, Brownlee M. Oxidative stress and diabetic complications. Circ Res 2010;107:1058–1070
11. Inoguchi T, Li P, Umeda F, et al. High glucose level and free fatty acid stimulate reactive oxygen species production through protein kinase C—dependent activation of NAD(P)H oxidase in cultured vascular cells. Diabetes 2000;49:1939–1945
12. Pleiner J, Schaller G, Mittermayer F, Bayerle-Eder M, Roden M, Wolzt M. FFA-induced endothelial dysfunction can be corrected by vitamin C. J Clin Endocrinol Metab 2002;87:2913–2917
13. Mishra R, Simonson MS. Oleate induces a myofibroblast-like phenotype in mesangial cells. Arterioscler Thromb Vasc Biol 2008;28:541–547
14. Huh KH, Ahn HJ, Park J, et al. Mycophenolic acid inhibits oleic acid-induced mesangial cell activation through both cellular reactive oxygen species and inosine monophosphate dehydrogenase 2 pathways. Pediatr Nephrol 2009;24:737–745
15. Brown FR 3rd, McAdams AJ, Cummins JW, et al. Cerebro-hepato-renal (Zellweger) syndrome and neonatal adrenoleukodystrophy: similarities in phenotype and accumulation of very long chain fatty acids. Johns Hopkins Med J 1982;151:344–351
16. Bonekamp NA, Völkl A, Fahimi HD, Schrader M. Reactive oxygen species and peroxisomes: struggling for balance. Biofactors 2009;35:346–355
17. Ho YS, Xiong Y, Ma W, Spector A, Ho DS. Mice lacking catalase develop normally but show differential sensitivity to oxidant tissue injury. J Biol Chem 2004;279:32804–32812
18. Elsner M, Gehrmann W, Lenzen S. Peroxisome-generated hydrogen peroxide as important mediator of lipotoxicity in insulin-producing cells. Diabetes 2011;60:200–208
19. Antonenkov VD, Panchenko LF. Effect of chronic ethanol treatment under partial catalase inhibition on the activity of enzymes related to peroxide metabolism in rat liver and heart. Int J Biochem 1988;20:823–828
20. Kino M. Chronic effects of ethanol under partial inhibition of catalase activity in the rat heart: light and electron microscopic observations. J Mol Cell Cardiol 1981;13:5–21
21. Wanders RJ, Ferdinandusse S, Brites P, Kemp S. Peroxisomes, lipid metabolism and lipotoxicity. Biochim Biophys Acta 2010;1801:272–280
22. Koepke JI, Wood CS, Terlecky LJ, Walton PA, Terlecky SR. Progeric effects of catalase inactivation in human cells. Toxicol Appl Pharmacol 2008; 232:99–108
23. Brezniceanu ML, Liu F, Wei CC, et al. Catalase overexpression attenuates angiotensinogen expression and apoptosis in diabetic mice. Kidney Int 2007;71:912–923
24. Brezniceanu ML, Liu F, Wei CC, et al. Attenuation of interstitial fibrosis and tubular apoptosis in db/db transgenic mice overexpressing catalase in renal proximal tubular cells. Diabetes 2008;57:451–459
25. Seo JY, Park J, Yu MR, Kim YS, Ha H, Lee HB. Positive feedback loop between plasminogen activator inhibitor-1 and transforming growth factor-beta1 during renal fibrosis in diabetes. Am J Nephrol 2009;30:481–490
26. Ha H, Yu MR, Choi YJ, Kitamura M, Lee HB. Role of high glucose-induced nuclear factor-kappaB activation in monocyte chemoattractant protein-1 expression by mesangial cells. J Am Soc Nephrol 2002;13:894–902
27. Hopfer U, Hopfer H, Meyer-Schwesinger C, et al. Lack of type VIII collagen in mice ameliorates diabetic nephropathy. Diabetes 2009;58:1672–1681
28. Ha H, Yu MR, Kim KH. Melatonin and taurine reduce early glomerulopathy in diabetic rats. Free Radic Biol Med 1999;26:944–950
29. Noh H, Kim JS, Han KH, et al. Oxidative stress during peritoneal dialysis: implications in functional and structural changes in the membrane. Kidney Int 2006;69:2022–2028
30. Oldfield MD, Bach LA, Forbes JM, et al. Advanced glycation end products cause epithelial-myofibroblast transdifferentiation via the receptor for advanced glycation end products (RAGE). J Clin Invest 2001;108:1853–1863
31. Gorin Y, Block K, Hernandez J, et al. Nox4 NAD(P)H oxidase mediates hypertrophy and fibronectin expression in the diabetic kidney. J Biol Chem 2005;280:39616–39626
32. Park J, Kwon MK, Huh JY, et al. Renoprotective antioxidant effect of alagebrium in experimental diabetes. Nephrol Dial Transplant 2011;26: 3474–3484
33. Goven D, Boutten A, Leçon-Malas V, Boczkowski J, Bonay M. Prolonged cigarette smoke exposure decreases heme oxygenase-1 and alters Nrf2 and Bach1 expression in human macrophages: roles of the MAP kinases ERK(1/2) and JNK. FEBS Lett 2009;583:3508–3518
34. Jiang T, Huang Z, Lin Y, Zhang Z, Fang D, Zhang DD. The protective role of Nrf2 in streptozotocin-induced diabetic nephropathy. Diabetes 2010;59: 850–860
35. de Haan JB, Stefanovic N, Nikolic-Paterson D, et al. Kidney expression of glutathione peroxidase-1 is not protective against streptozotocin-induced diabetic nephropathy. Am J Physiol Renal Physiol 2005;289:F544–F551
36. Bagattin A, Hugendubler L, Mueller E. Transcriptional coactivator PGC-1alpha promotes peroxisomal remodeling and biogenesis. Proc Natl Acad Sci U S A 2010;107:20376–20381
37. Finkel T, Holbrook NJ. Oxidants, oxidative stress and the biology of ageing. Nature 2000;408:239–247
38. Lee HC, Wei YH. Mitochondrial biogenesis and mitochondrial DNA maintenance of mammalian cells under oxidative stress. Int J Biochem Cell Biol 2005;37:822–834
39. Cochemé HM, Quin C, McQuaker SJ, et al. Measurement of H2O2 within living Drosophila during aging using a ratiometric mass spectrometry probe targeted to the mitochondrial matrix. Cell Metab 2011;13:340–350
40. Thoms S, Grønborg S, Gärtner J. Organelle interplay in peroxisomal disorders. Trends Mol Med 2009;15:293–302
41. Baumgart E, Vanhorebeek I, Grabenbauer M, et al. Mitochondrial alterations caused by defective peroxisomal biogenesis in a mouse model for Zellweger syndrome (PEX5 knockout mouse). Am J Pathol 2001;159:1477–1494
42. Goldfischer S, Moore CL, Johnson AB, et al. Peroxisomal and mitochondrial defects in the cerebro-hepato-renal syndrome. Science 1973;182:62–64
43. Proctor G, Jiang T, Iwahashi M, Wang Z, Li J, Levi M. Regulation of renal fatty acid and cholesterol metabolism, inflammation, and fibrosis in Akita and OVE26 mice with type 1 diabetes. Diabetes 2006;55:2502–2509